



# An investigation of the applicability of SPIV for the analysis of the dynamics of floating offshore wind platforms

Navid Belvasi<sup>1, 2, \*</sup>, Frances Judge<sup>1</sup>, Jimmy Murphy<sup>1, 2</sup>, Brian Flannery<sup>1</sup>, Cian Desmond<sup>3</sup>

<sup>1</sup> MaREI, Environmental Research Institute, University College Cork, Cork, Ireland

<sup>2</sup> School of Engineering, University College Cork, Cork, Ireland

<sup>3</sup> Head of Innovation, Gavin & Doherty Geosolutions Ltd., Dublin, Ireland

\*Corresponding author: Navid Belvasi ([nbelvasi@ucc.ie](mailto:nbelvasi@ucc.ie))

## Abstract

There is a need for new numerical tools to capture the physics of floating wind platforms more accurately to refine engineering designs and reduce costs. The conventional measurements apparatus in tank tests, including wave probs, velocity and current profiler, as well as doppler sensors, are unable to give a full 3D picture of velocity, pressure, and turbulence. In tank testing, the use of the underwater stereoscopic PIV method to fully characterise the 3D flow field around floating platforms can provide a rich source of validation data and overcome some of the limitations associated with more classical measurement techniques. This optical technique can be used to accurately measure the random and chaotic structure of turbulent flows around the floater. Moreover, the main characteristics of turbulence of the flow around the floater, such as rotationality, diffusivity, irregularity, as well as dissipation, can be extracted and studied. The underwater S-PIV method has been widely used for marine and offshore applications, including studies on ship and propeller wakes and tidal stream turbines; however, to date, this technology has not seen widespread use for the hydrodynamic study of floating offshore wind turbines. Therefore, in the current study, the key considerations for using S-PIV for this purpose are discussed; meanwhile, the related studies in the field of quantitative flow measurements are reviewed.

Keywords: Floating offshore wind turbine, Stereoscopic particle Image velocimetry, SPIV, experimental campaign, tank testing, measurement techniques



## 25 **1 Introduction**

Considering the 30 MW Hywind Scotland, the 24 MW WindFloat project in Portugal and upcoming projects including 30 MW EFGL in France and 88 MW Hywind Tampen (WindEurope, 2020), Europe is on course to become a world leader in floating offshore wind. Current estimations for floating offshore wind turbines (FOWTs) suggest that the cost of energy will fall by 70% and reach 40 Eur/MWh by 2050, while total installed capacity is expected to increase to 250 GW (DNV GL, 2020). However, these cost reductions are not guaranteed and will require robust design tools to enable designers to balance cost reduction, structural integrity, and project risk. A wide variety of engineering design tools with a limited representation of the underlying physics have been developed and employed for FOWT design (Cordle and Jonkman, 2011). A comprehensive review of the current state of the art of numerical tools in the field of FOWTs was carried out in press (Otter et al., 2021).

35 These numerical codes are based on either the frequency or time domains analysis. As low fidelity models, the frequency-domain codes utilise strip theory, panel method, or a combination of both. While this approach provides shorter CPU time, a limited capacity to capture the low-frequency motion of the floating platform result in inconsistencies and error. These errors could be up to a 20% difference in the mean value of the results (Rahimi et al., 2016). Conversely, time-domain codes, including full Computations Fluid Dynamics (CFD) simulations, provide a more complete picture of platform responses as nonlinearity is considered. Such CFD codes provide high fidelity data such as turbulent kinetic energy, velocity distribution, flow wakes, as well as the wave-making characteristics of floater (Liu et al., 2017). Accurately capturing turbulence modelling is essential for response analysis of the floater so that the engineers can produce reliable and cost-effective designs in terms of fatigue load estimation and structural and mooring design of FOWTs.

45 In CFD, turbulence modelling involves a mathematical model that estimates the effects of turbulence on fluid flow. Although there is no analytical theory to predict turbulent flows, many researchers have numerically studied turbulence formation, and several hybrid models have been developed. A review on the state of the art of hybrid turbulence models is conducted by (Chaouat, 2017). In respect of turbulence modelling, the CFD codes provide high fidelity data, such as Reynolds stresses, specific dissipation rate (SDR), turbulent kinetic energy (TKE), along with TKE production and dissipation rate (TDR). Standard turbulence models for these numerical codes are



55 *Spalart–Allmaras*,  $k-\varepsilon$ <sup>1</sup>,  $k-\omega$ <sup>2</sup>, *SST*<sup>3</sup>, and RSM<sup>4</sup>. Alongside, some researchers favour the use of LES<sup>5</sup> approach to fully simulating the turbulent structures of the flow. These high-fidelity numerical approaches have a significant computational expense compared to linearised engineering models however, their use will be required to resolve detailed flow phenomenon and system response. There is a requirement for validation data to reduce inaccuracies and errors in these high-fidelity numerical simulations. A study on the accuracy of turbulence models was undertaken by (Rezaeiha et al., 2019), which reveals that uncertainty levels for demonstration of a model’s wake in fluid flow could reach 30% near the wall of the model.

60 In both frequency and time domain approaches, there is a lack of accurate verification data. As the technologies advance, high fidelity models will see greater adoption. Moreover, the validation of these advanced models will be critical. Tank testing and real-world demonstrations are sources of validation data, though higher accuracy measurement apparatus is required to fully resolve flows and response. In tank tests, the single-point wave measurement equipment includes wave probes, laser doppler velocimeters (LDV), as well as acoustic doppler velocimeters (ADV). Additionally, for current measurements, there are velocity profilers such as Acoustic Doppler Current Profiler (ADCP), as well as hot wires or pitot tubes. These are practical tools to measure fluid velocity only  
65 at individual points in the tank. Moreover, these pieces of experimental equipment have their associated errors; a comprehensive review of underwater speedometer equipment and its measurements error is conducted by (Fuentes-Pérez et al., 2018). Using only these instruments, it is impossible to fully and accurately understand the tank’s flow regime, for instance, full velocity and pressure distribution contour; and so, a complete 3D picture of the fluid flow cannot be produced for the validation of high-fidelity numerical models.

70 Comprehensive flow characterisation can be achieved by stereoscopic particle image velocimetry (S-PIV). The S-PIV is an optical measurement technique where the velocity field of an entire region within the flow is measured simultaneously. This is the fundamental advantage of S-PIV against single point measurement methods. S-PIV facilitates both the extraction of measurement data and the visualisation of flow structures. An optical non-intrusive technique allows a complete picture of the turbulent flow field to be produced; it reveals insights about the study

---

<sup>1</sup> K-epsilon

<sup>2</sup> K-omega

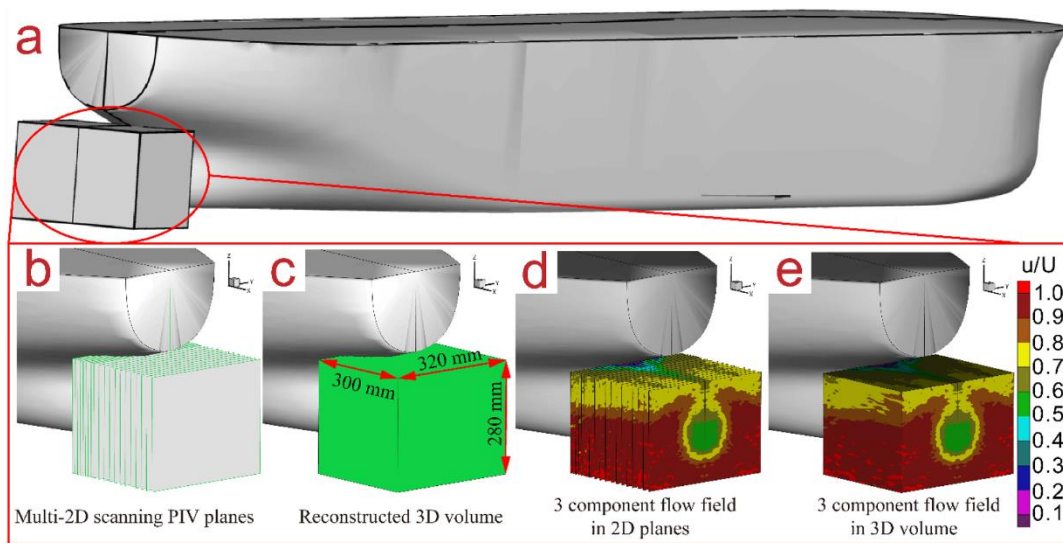
<sup>3</sup> Menter’s Shear Stress Transport

<sup>4</sup> Reynolds stress equation model

<sup>5</sup> Large Eddy simulation



75 domain, for instance, velocity, turbulent kinetic energy, and vorticity distribution. Moreover, as a high-fidelity method, the resolution of data captured by S-PIV is equivalent to several thousand measuring points in an assumed interrogation window (See Figure 1). Therefore, in an assumed spatial volume, the fluid flow parameters can be measured with high resolution.



80

**Figure 1 Reconstruction procedure of 3D-3C flow with multiple 2D-3C SPIV velocity planes: a) Interested area at the model aft; b) Locations of multiple-2D scanning SPIV planes; c) Reconstructed 3D volume; d) 3 Component flow field in 2D planes; e) 3D component flow field (Wu et al., 2020)**

85 The S-PIV technique is widely used for studying the aerodynamics of offshore wind turbines (Figure 2), e.g. (Bayati et al., 2018), (Xiao et al., 2011), (Wang et al., 2015) and for the validation of complementary CFD simulations (Desmond et al., 2014). Additionally, some researchers use the S-PIV technique to study other marine renewable technologies (Day et al., 2015); however, the use of underwater S-PIV for FOWT's tank testing is an emerging field. This method can be used to fully characterise the 3D flow field around floating platforms in the laboratory  
90 environment, provide a rich source of validation data and overcome some of the limitations associated with conventional measuring equipment of fluid flow (Chen et al., 2020).

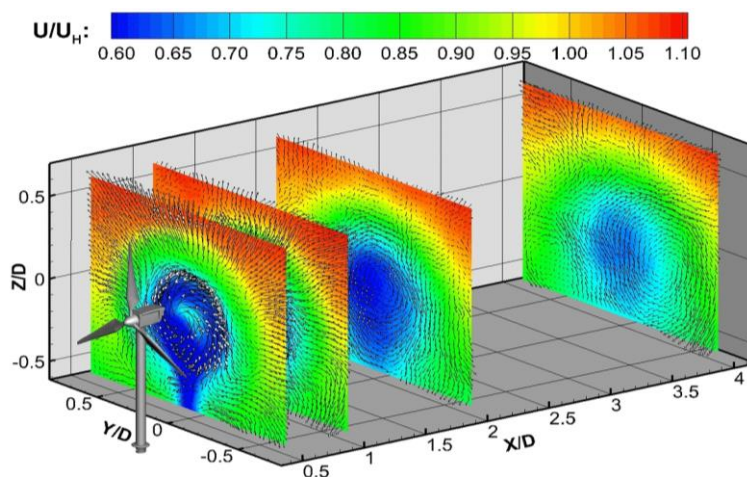


**Figure 2** Stereoscopic PIV measurements of a wind turbine wake (Wang et al., 2015)

95 This technique has not seen widespread use in FOWT tank test campaigns to date. This paper reviews state of the art in S-PIV techniques and identifies opportunities for their use in tank test campaigns to better understand the flows around the floater and to provide a rich source of validation data for advanced numerical models. Despite the high-resolution results of S-PIV, there are uncertainties associated with the laser frequency, tracer particle response, and hardware synchronisation in each test case. Therefore, to utilise this technology for the hydrodynamics of FOWTs, there are various errors, uncertainties, and quantitative parameters to be studied. This review paper covers the vast majority of these parameters in the following section and discusses the relevant research in the field of quantitative flow visualisation.

## 2 The S-PIV, its application, and challenges for FOWT tank testing

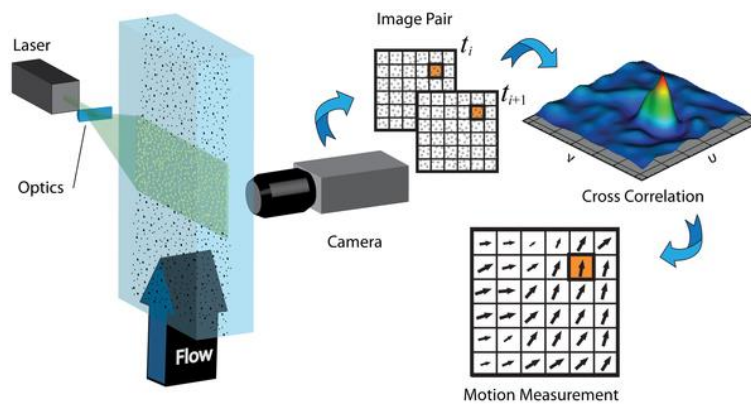
### 2.1 Theory of Particle Image Velocimetry

105 The basis of PIV is the measurement of particles' displacement at different time steps. The fluid flow is filled with traceable particles; then, a laser light passed through a lens becomes a flat light sheet and illuminates these particles. The PIV measurement is achieved by group tracking of fluid particles and processing their trajectory at different time intervals. By high-frame imaging of the illuminated particles and post-processing of consecutive images, the particle group's displacement is extracted for each time step, and their relative velocities are calculated using a group distance and a sample time (See Figure 3). This travelling distance depends on parameters such as flow rate,

110



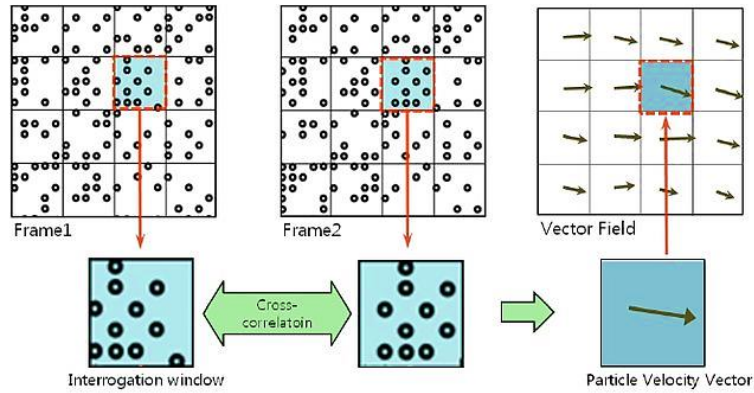
camera frame rate, as well as the level of fluid flow turbulence. Since this method is an indirect measurement, the movement of tracer particles within the fluid flow is examined instead of determining the flow attributes. Therefore, the type of particle seeds and their properties are chosen based on the studied fluid and turbulence.



115 **Figure 3 Schematic description of the PIV principle** (Ismadi et al., 2013)

Various methods such as Gaussian, phase discrimination and Dynamic Mean Value Operator have been developed to review and post-process the PIV raw data (Markus, Raffel, Christian E. Willert, Fulvio Scarano, 2018). These image comparison methods can later be distinguished from each other in their local or global regularisation schemes. Global schemes iteratively optimise the entire flow field and its displacement path, while in the local methods, a number of interrogation windows are selected, and the group path of particles inside these windows are investigated in the consecutive images (See Figure 4). This iterative phase is repeated for all captured images in the interrogation windows. A well-known approach to conduct this iterative step is to use the cross-correlation method. The cross-correlation method is used commonly in particle image velocimetry.

120



125

**Figure 4** Two frames cross-correlation PIV (Choi et al., 2011)

130

A review of the theory of the cross-correlation method and its application in particle image velocimetry has been conducted by (Keane and Adrian, 1992). Based on this method, if the parameter  $D$  is considered the constant displacement of all particles in an interrogation window, then particle locations at the next time step are given by Equation (1).

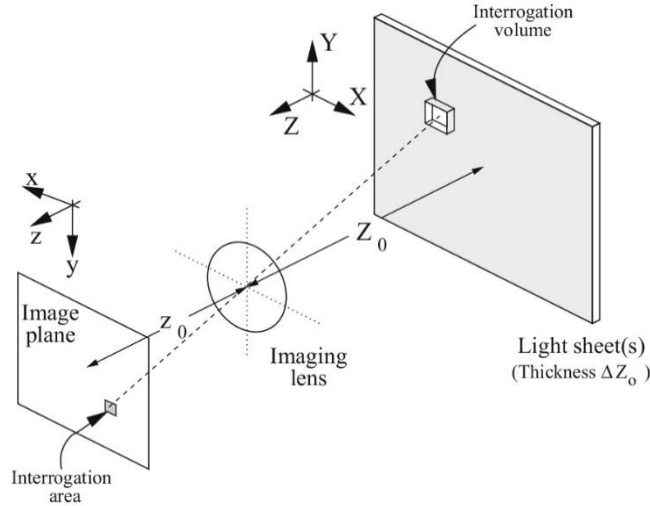
$$X'_i = X_i + D = \begin{pmatrix} x_i + D_x \\ y_i + D_y \\ z_i + D_z \end{pmatrix} \quad (1)$$

Moreover, by assuming the particle image displacement given by Equation (2), the image intensity for the second step is calculated from Equation (3).

$$d = \begin{pmatrix} M \cdot D_x \\ M \cdot D_y \\ M \cdot D_z \end{pmatrix} \quad (2)$$

$$I'(x, \Gamma) = \sum_{j=1}^N V'_0(X_j + D) \tau(x - x_j - d), \quad (3)$$

where  $V'_0(X)$  defines the interrogation volume during the second time step (see Figure 5).



135

**Figure 5 Imaging of light sheet in Particle image velocimetry** (Markus, Raffel, Christian E. Willert, Fulvio Scarano, 2018)

If the light sheet and the windowing characteristic are assumed identical for images in two consecutive time steps, the cross-correlation function of the interrogation area can be written as:

$$R_{II}(s, \Gamma, D) = \sum_{i,j} V_0(X_i) V_0(X_j + D) R_\tau(x_i + x_j + s - d), \quad (4)$$

140

Where  $V_0$  is the interrogation volume, and  $s = (x, y)$ ,  $s_D = M \cdot (\Delta x, \Delta y)$  is the particle tracer displacement on the image. The  $i \neq j$  terms represent the correlation of different randomly distributed particles, so, they are mainly the noise in the correlation plane. Moreover, the  $i = j$  terms are the desired displacement information. With distinguishing the noise from the desired displacement information, the cross correlation function is given by Equation (5).

$$\begin{aligned}
 R_{II}(s, \Gamma, D) = & \sum_{i \neq j} V_0(X_i) V_0(X_j + D) R_\tau(x_i + x_j + s - d) \\
 & + R_\tau(s - d) \sum_{i=1}^N V_0(X_i) V_0(X_i + D)
 \end{aligned} \quad (5)$$

145

Therefore, the component of the cross-correlation function correspond to particle image is as (6).

$$R_D(s, \Gamma, D) = R_\tau(s - d) \sum_{i=1}^N V_0(X_i) V_0(X_i + D) \quad (6)$$



Hence for a given number of particles inside an interrogation window, the maximum displacement correlation peak that can be reached is at  $s = d$  (see Figure 6). The location of this correlation peak is representative of the maximum particles group displacement. The cross-correlation method enables us to locate the particles groups in each time step; so that having the time step and particles group displacement results in having the velocity vectors and contours.

150

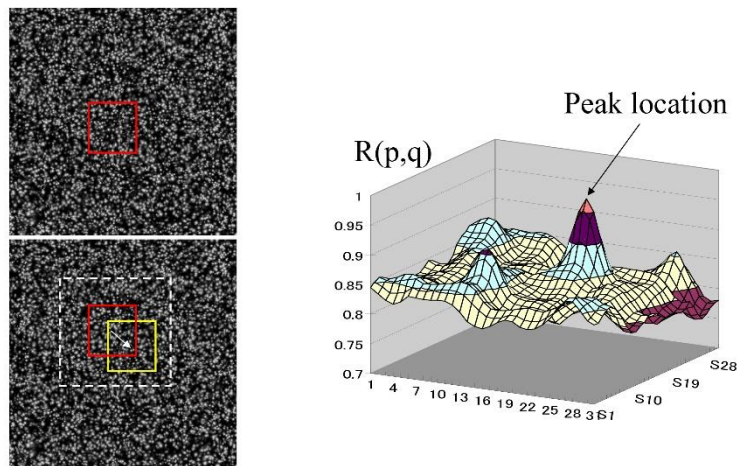


**Figure 6** Correlation peak of an assumed interrogation window in two consecutive images (Markus, Raffel, Christian E. Willert, Fulvio Scarano, 2018)

## 155 2.2 State of the art of Particle Image Velocimetry in tank tests

PIV was first used for tank testing by Dong (Dong et al., 1997). The main motivation of this research was to wave structure near the bow of a ship model. The test was performed using a camera and an underwater light sheet. After processing the data, the researchers extracted a two-dimensional velocity field for a 3.05 m ship model in flow with a Froude number in the range of 0.17 to 0.45. These measurements also determined the velocity near the free surface. In this research, a special focus was on flow vorticity production and its energy losses. This result was significant as the PIV method revealed the turbulence intensity and the 3D velocity distribution in the tank test campaign (see Figure 7).

160

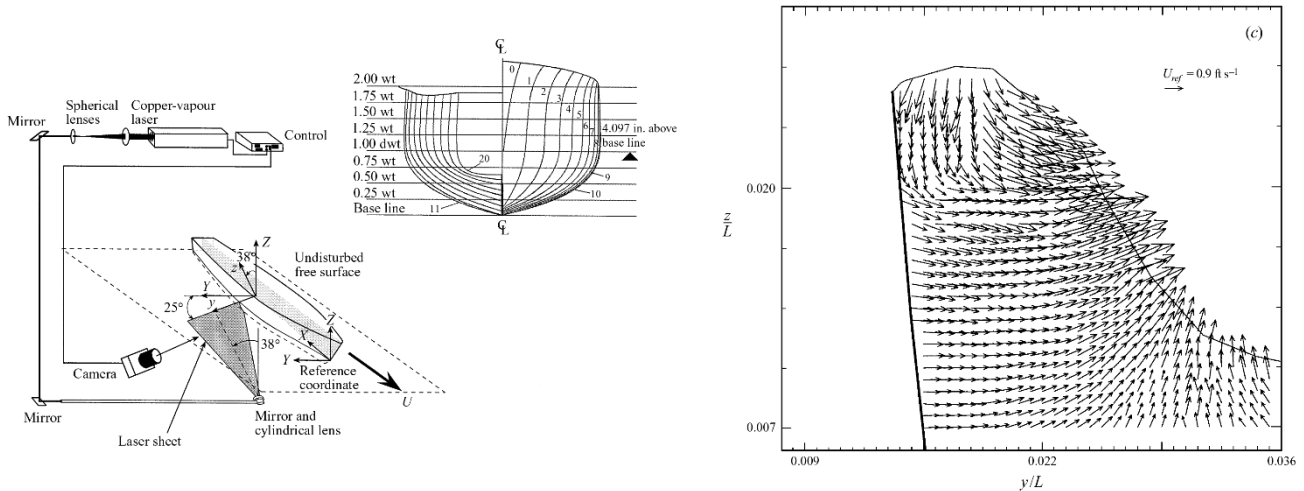


**Figure 7** From the left: Dong's PIV setup, Magnitude portion of the velocity field (Dong et al., 1997)

165

Another study was performed by by Tukker *et al.* (Tukker et al., 2000). The motivation of the research was to study the feasibility of using the PIV technique to measure the unsteady spatial structure of flow in test tanks. Attention was paid to the main features of PIV in test tanks, including the seeding of a large quantity of water, the visibility of the particle in water, as well as measuring the accuracy of the method. For the first time, a digital camera was used for PIV in a test tank. A 64x64 pixels interrogation window was used to record the wake area behind a passing ship model. The PIV equipment was stationary, which limited the study to examining only one area of the ship's path. However, the study result was beneficial since it could visualise the unsteady and spatial flow dynamics around a model. Tukker's study shows that using a higher-resolution digital camera increases the frame accuracy and quality of data for the two-dimensional plane. Using this method in a tank test was promising since it could record the instantaneous flow velocity measurements. However, the use of 2D PIV causes out off-plane velocity error, which is the calculation errors for the velocity vectors in the third dimension normal to the light sheet.

170

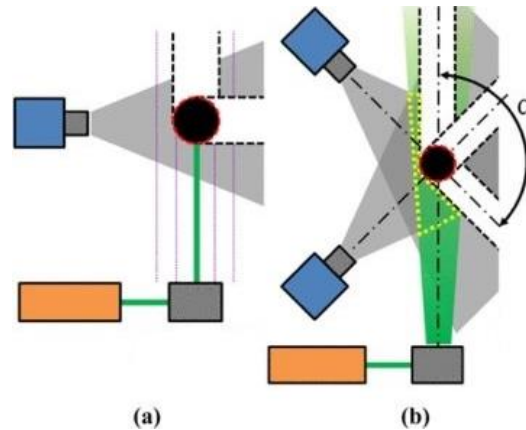
175

In the research described above, all PIV experiments only recorded two-dimensional velocity vectors, and the error in the third dimension was due because of the particles leaving the thin light sheet. This error in the third dimension is known as the ubiquity problem. This is a disadvantage since the flow structure after the model has a significant 3D characteristic. In the single-camera method, the particle velocity can be calculated correctly only in two dimensions on the laser screen. In the S-PIV method, the particle velocity in the third dimension can also be obtained by post-processing of vectors (Baghaie, 2019). Therefore, by having the corresponding images recorded

180



by the two cameras, the actual velocity vector in the third dimension can be calculated with a geometric reconstruction (see Figure 8).

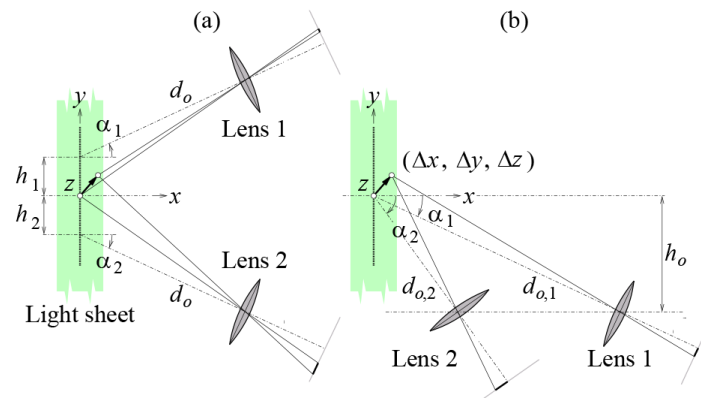


185

**Figure 8 Comparing PIV and S-PIV technique to solve the ubiquity problem for the out of plane vectors** (Jux et al., 2018)

An important parameter in the S-PIV test is the angle of cameras relative to the light sheet. Lee *et al.* conducted a sensitivity analysis (Lee et al., 2014) for different camera angles in the S-PIV method. They extracted the maximum value of error related to in-plane and out-of-plane velocity vectors for different cameras angles (see Figure 9). The research shows that the ideal camera angles are symmetric 45 degrees to the light sheet, which may not be suitable for all test campaigns depending on the dimensions of the model and the dimensions of the basin or the cameras' distance to the illuminated plane.

190



195

**Figure 9 symmetric and asymmetric camera angle in an S-PIV test** (Lee et al., 2014)



Research was conducted on various types of S-PIV systems with different arrangements consisting of two vertical cylinders (Egeberg et al., 2014). The purpose of the experiment was to study the generated vortex of a 3.047 m ship model. The new design allowed for the capture of vortices with a frequency of 3 Hz. The distribution of velocity and vorticity are used to characterise vortices. Since the PIV method can capture and visualise the instantaneous velocity and vorticity field, the vortex in the fluid flow can be captured simultaneously. Having an accurate estimation of vortex around the model can improve the design to reduce undesired phenomena such as vortex-induced vibration and motion (VIV, VIM), multi-body flow interaction, wave-current body interaction, sloshing, as well as the instantaneous position of wave load. Additionally, this estimation can lead to a better understanding of flow wake around the floater model, which leads to an accurate estimation of floater motion in different environmental conditions.

S-PIV equipment is widely used in marine engineering applications since it can provide high fidelity results of applied force on the model. Lee *et al.* examine the wave field of a containership model (Lee et al., 2009). Their velocimetry measurements were at four different sections of the model, using CCD cameras<sup>1</sup> with a resolution of 1024x1024 pixels. Utilising the S-PIV technique enabled the extraction of velocity and vorticity distributions to capture phenomena such as counter-rotating vortices in the model's wake area. The result of this study characterised the near-wake region for the model. Different counter-rotating longitudinal vortices, their location, as well as their trajectories were also determined. Another achievement of this S-PIV-based experimental campaign was finding the vortex's centre in different loading conditions. This facilitates an examination of the inflow condition and a clear picture of the turbulent intensity distribution and its vortices in the wake area of the model (see Figure 10).

---

<sup>1</sup> Charge-coupled device camera (Anthony F. Molland, 2008)

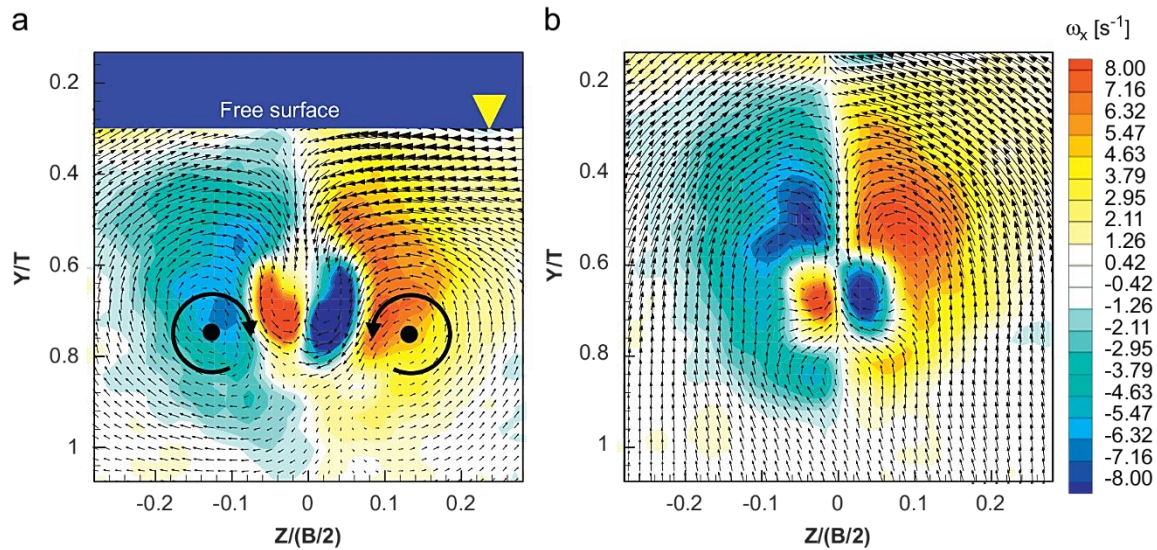
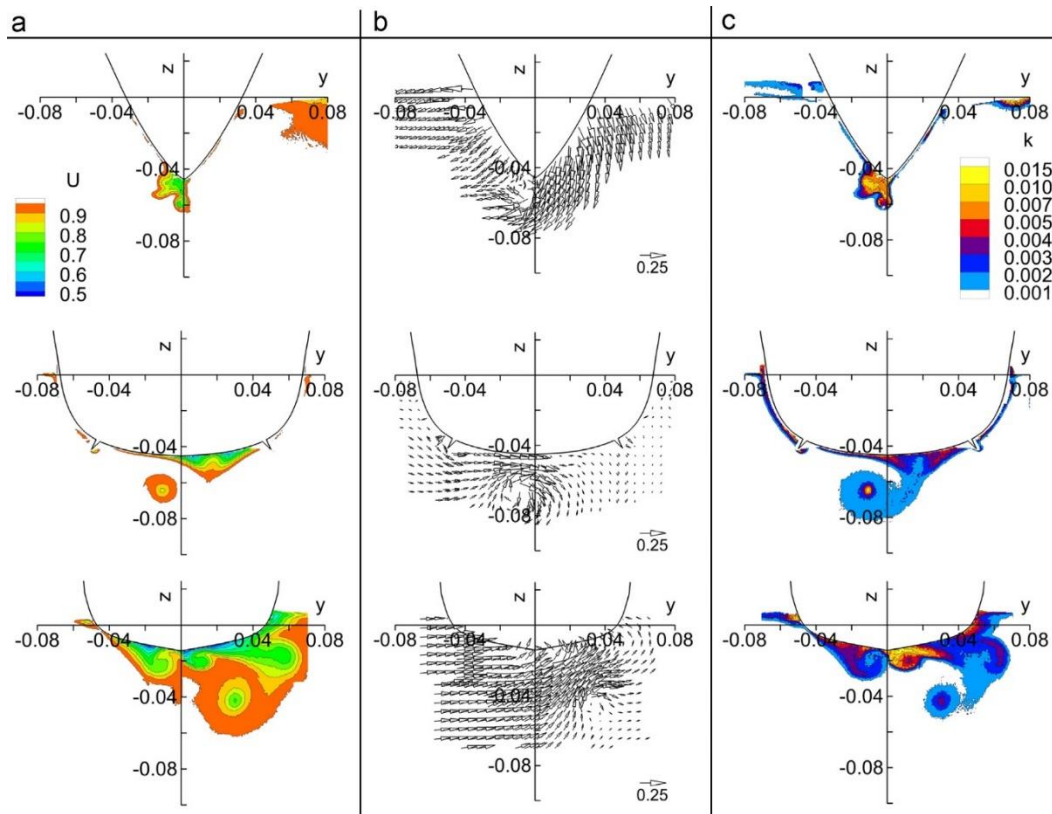


**Figure 10** Mean velocity and vorticity as  $St=0.591$  for a model ship at  $(X/L_{pp}=0)$  for a. ballast load case b. full load case (Lee et al., 2009)

220

S-PIV is a suitable tool for studying turbulence flows; however, it is critical to limit the uncertainty of the method in test campaigns. Yoon et al. carried out a benchmarking investigation by examining a ship model with a length of 3.048 m using the S-PIV system. The first aim of the research was to create a manoeuvre database for that model (Yoon et al., 2015). The second aim was to develop a systematic method for examining the S-PIV uncertainties, setting the validity criteria on converging error and performing a standard uncertainty assessment. The test campaign was carried out for pure yaw and sway tests. Moreover, the result included the axial velocity and turbulent kinetic energy at the measurement sections (See Figure 11). The convergence error of their test campaign was less than 1% of the towed velocity  $Uc$  for the velocity distribution field. Additionally, their standard uncertainty was in the range of 2-3%  $Uc$  for the velocity fields.

225



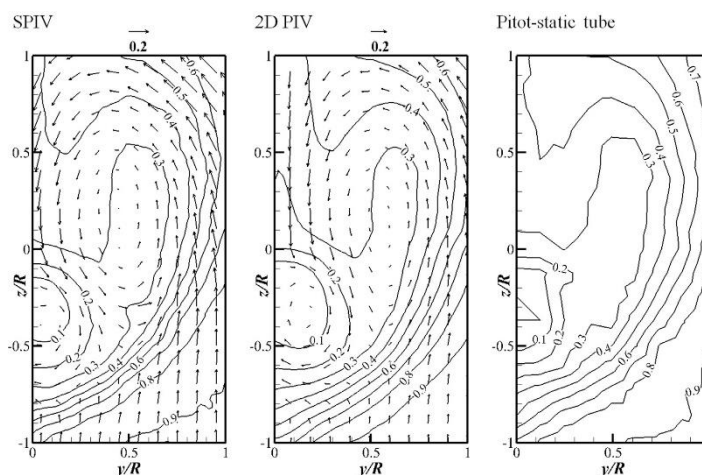
230

**Figure 11 Pure yaw test: a. Axial velocity, b. cross-plan VW-vectors, c. turbulent kinetic energy (Yoon et al., 2015)**

235

240

In the underwater S-PIV technique, the equipment, including cameras and laser, are kept underwater. These attachments may influence the flow regime by causing backflow and interaction with the flow around the model. This issue is examined by Han et al., who investigated the uncertainties of the S-PIV method for its application in the tank test (Han et al., 2018). A ship model with a Froude scale of 1/100 in both uniform flow and nominal wake flow was studied. Two 14 Hz digital cameras were used to undertake the detailed examination. In order to quantitatively assess the high fidelity results, the proposed procedure of ITTC (ITTC, 2008) and the proposed method of Yoon's research (Yoon et al., 2015) was utilised. In their experiment, it was found that the torpedo configuration of the S-PIV system does not significantly affect the computational velocity field and the resulting error was negligible. The nominal wakefield measured in that research is shown in Figure 12. The research showed that data obtained with the S-PIV technique are both accurate and high resolution. Moreover, the equipment in this technique does not interfere with the fluid flow.



245 **Figure 12** Nominal wakefields for a model in different measuring techniques (Contour lines is  $\bar{u}$  and the vectors is tangential velocity components)

To date, the use of underwater S-PIV in tank tests has been limited to the study of ship propellers (Go et al., 2019), tidal stream turbines (Seo et al., 2016), the ship model wave field (Mallat et al., 2015), (Jacobi et al., 2016), (Tukker et al., 2000) and basic phenomena such as vortex-induced vibrations (Ashworth Briggs et al., 2019). There are successful attempts in the literature to use this technology to create a high-fidelity ship manoeuvring database (Yoon et al., 2015). The same approach can be used for the hydrodynamic study of FOWT with regard to minimising the uncertainty of velocity measurements in the test campaign. The high-resolution data of vorticity, full velocity distribution and turbulent kinetic energy then can be used as a source of validation data for numerical codes for FOWTs.

250

255



### 3 Critical parameters of underwater S-PIV

The most critical issues in using S-PIV underwater and in the wave-basin are the type of seeding particles, out of plane velocity of particles, illumination in water, imaging technique, different camera angles and the associated uncertainties. These critical parameters are discussed in this section.

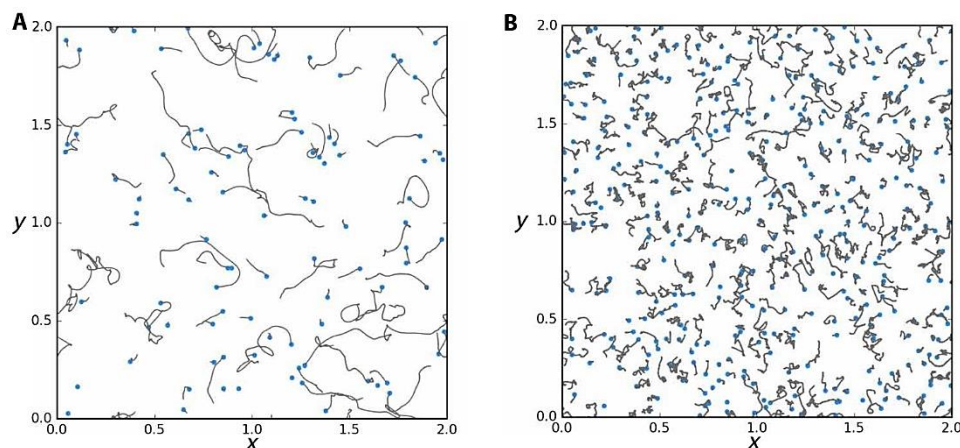
The study area in the tank test usually has a significant three-dimensional turbulent characteristic. Many parameters such as image pixel size, particle strength and density, velocity gradients, turbulence variation, and noise level (Scharnowski and Kähler, 2016) are involved in error generation and raising the uncertainty of this method. In the previous two decades, researchers have tried to identify and reduce these errors sources (Sciacchitano, 2019), (Markus, Raffel, Christian E. Willert, Fulvio Scarano, 2018), (Kähler et al., 2012), (Charonko and Vlachos, 2013), (Bhattacharya et al., 2018), (Neal et al., 2015). One of the well-known methods is uncertainty surface (Timmins et al., 2012), in which captured images are analysed for parameters affecting the error.

#### 3.1 Particle seeds

The S-PIV technique is an indirect approach, so instead of directly examining the flow, the response of illuminated particles in the flow is analysed. Therefore, in particle selection, the particle mass and the optical reflectance are important. In seeding selection, other factors such as the distribution of particles and the seeding density in the fluid should also be studied for each test; these criteria have been well studied in (Markus, Raffel, Christian E. Willert, Fulvio Scarano, 2018).

The primary sources of error are the effect of gravity and buoyancy on the motion and response of particles. Particles with lower density than the fluid follow the fluid path very well (See Figure 13). However, the cumulative effect collisions between particles and the fluid vortex cause unwanted random movement of the particles. This random motion is called Brownian motion (Olsen and Adrian, 2000), leading to measurement error up to 15% of fluid flow velocity (Catipovic et al., 2013). Contrarily, coarse particles with a density higher than fluid do not respond well to fluid flow turbulence (Al-Muhammad et al., 2018).

The reflectivity of the particles is another topic of interest. Coated glass particles are commonly used in underwater PIV testing. Their uniform dimensions and excellent reflectivity attributes made them suitable for underwater application. However, in typical wave basins (Desmond et al., 2016), the need for high quantities of particles for several tests makes the coated glass an uneconomical option.



285 **Figure 13 Trajectories of vortices, A. course seeding  $Ek = 1 \times 10^{-4}$  B. dense seeding  $Ek = 7 \times 10^{-6}$**  (Chong et al., 2020)

Fluorescent particles can also be used, as they avoid unwanted reflection of the model surface and bubbles. However, these particles are expensive. A suitable alternative is Orgasol and Vestosint particles (Schröder et al., 2020), which have the same reflectance quality and good economical efficiency. Ashworth Briggs *et al.* have recently proposed a practical alternative to these conventional particles during their test campaigns (Ashworth Briggs et al., 2019). In that research, a series of fluorescent particles with 57  $\mu\text{m}$  mean diameter were fabricated and coloured with Rhodamine 6G. In this research the uncertainty of the experiment is reduced to 0.5  $\mu\text{m}$ . In particle selection, other factors such as the distribution of particles and the seeding density in the fluid should also be studied for each test; these criteria have been well studied in (Markus, Raffel, Christian E. Willert, Fulvio Scarano, 2018).  
290  
295 Nonetheless, choosing the right particles are based on test condition and the understudied phenomenon.

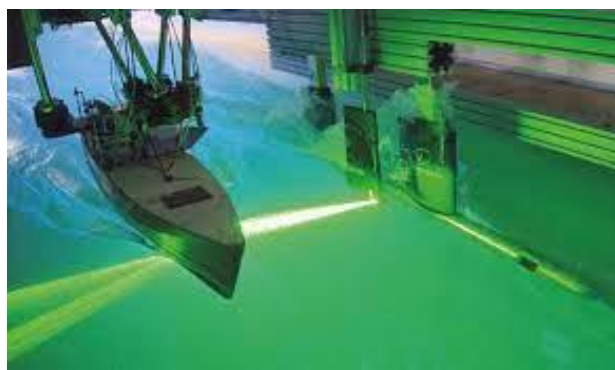
### 3.2 Illumination

Lasers are one of the integral components of PIV tests. These elements create monochromatic light with high energy density. Passing this light through an optic lens turns it into a thin light sheet (See Figure 14), which illuminates the particles. In comparison with aerodynamics, in hydrodynamics, the fluid is denser, and it is necessary to use high power lasers for illumination. For the first PIV experiments, a 20 MJ laser was used in the tank test described by (Dong et al., 1997); more recently, ND YAG lasers provide illumination power up to 200 MJ at a wavelength  
300



of 532 nm (Abdulwahab et al., 2020). At this maximum energy, the maximum repetition frequency is within the range of 7-25 Hz.

305 The laser frequency must be synchronised with the camera shooting frequency, and the repetition rate of the laser radiation should be adjusted according to the imaging rate (Jacobi et al., 2016). For example, a laser with a power of 200 MJ has an approximate repetition frequency of 20Hz; if a higher frequency is needed, the laser power should be decreased. However, this results in less illumination in the water medium and lower image quality.

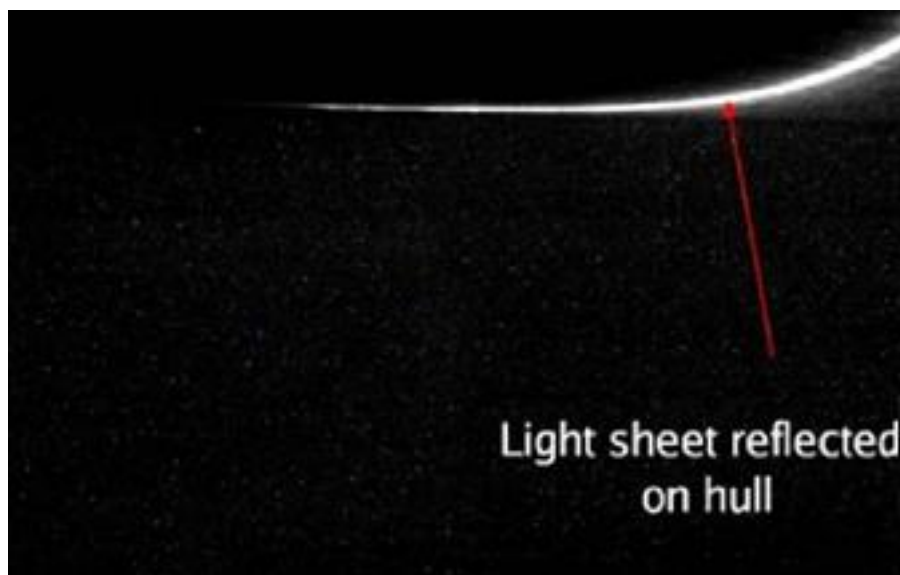


310

**Figure 14 Stereo-PIV system in a towing tank** (Jacobi et al., 2016)

315

Another issue is the high reflection from the model surface in the water environment (see Figure 15), which is due to the high laser illumination. Reflection problems at or near the model wall boundary due to high laser illumination can lead to errors and has been examined in various studies. Sciacchitano investigated the reduction of errors in this area as well as the overall reduction of method uncertainty (Sciacchitano, 2019). A comprehensive methodology for studying this error and introducing approaches to prevent it in a PIV campaign is given by (Adrian et al., 2011). A possible solution to this issue is to paint the model black or fabricate the model using acrylic material. However, it is not possible to made complex models out of these materials.



320

**Figure 15 Reflection issue because of high illumination** (Grizzi et al., 2010)

In the PIV method, the velocity components are usually calculated on a two-dimensional light sheet. Using only one camera results in a perspective error as any out of the plane movement of particles leads to an error in calculating the third-dimension vectors (Ajay K. Prasad, 2000). This error is reduced using the S-PIV method (two cameras), although the accuracy of the results may still be affected since the technique is based on 2D assumption, and any particle motion vector outside the particle plane affect the results.

325

330

Several particles that move across the illuminated light-sheet could affect the light sheet's intensity in different images. The particles disappear when leaving the light sheet, and the new particles are replaced constantly; this affect the post-processing schemes' error (Wieneke, 2017). This random error is one of the fundamental and dominant errors in the S-PIV method. A recommended approach to mitigate this error is to ensure that less than a quarter of the particles leave the light sheet between each two laser pulses (Adrian et al., 2011).

335

In order to limit out of plane loss, (Markus, Raffel. Christian E. Willert, Fulvio Scarano, 2018) propose several methods for recording particle path; however, each of these methods has its own advantages and disadvantages. One approach is to divide the time interval between pulses. The velocity is obtained by reconstructing the movements in a time interval (Zhong Li, Jinwei Ye, Yu Ji, Hao Sheng, 2019). Therefore, this method reduces the fluctuations of the constructed velocity field both in the third dimension and on the light sheet plan.



### 3.3 CCD cameras and image processing

340 The advantage of the S-PIV over the PIV method is using two digital cameras instead of one camera; thus, the third velocity vector is calculated correctly with a geometrical reconstruction of images, and the associated error is reduced. However, the presence of two cameras with different angles leads to a loss of a part of the interrogation window. Moreover, the lenses' angle and the requirement for a mapping technique results in a relative error in the overall calculation of the velocity field.

345 Various arrangements for the two cameras have been suggested by (Markus, Raffel, Christian E. Willert, Fulvio Scarano, 2018). However, a 45-degree angle is an optimal angle in terms of error reduction to error ratio of 1 percent (Lee et al., 2014). Jurgens *et al.* have also investigated this issue in their study (Jurgens, 2007) and proposed a symmetrical setup for two cameras to reduce the error. Although this type of arrangement usually has the least error for the third velocity vector, it strongly affects the vector and fluid distribution around the model. In any case, the dimensions of the model, tank test, and the interrogation window are the three primary parameters that set the distance and angle of the cameras to the light sheet.

350 After capturing the raw image data, there are a significant number of outliers, and the raw data needs to be pre-processed. Image processing in the S-PIV method usually has three main phases (Garcia, 2011): (1) Data validation and velocity vectors (outliers) extraction, (2) Replacement scheme, and (3) Data assimilation. A comprehensive review of many of these pre-processing algorithms' advantages and disadvantages has been carried out by (Westerweel et al., 2013). Many researchers have worked on optimising these algorithms (Liu et al., 2008); however, one of the most valid methods for this purpose is the global histogram filter (Pun et al., 2007).

360 Researchers have worked on developing different schemes to investigate the uncertainty of S-PIV and the parameters that have the greatest impact on uncertainty. Among the well-known and widely used methods, we can mention the uncertainty surface method (Timmins et al., 2012), multi-pulse and multi-frame (Westerweel et al., 2013), particle disparity (Sciacchitano, 2019), and peak ratio method (Charonko and Vlachos, 2013). These schemes and their governing mathematical equations have been thoroughly discussed and reviewed in (Sciacchitano, 2019), (Markus, Raffel, Christian E. Willert, Fulvio Scarano, 2018), (Wieneke, 2017), (Adrian, R. J. and Westerweel, 2011).



365 **4 Application of underwater S-PIV for tank testing of FOWTs**

There is a variety of hydrodynamical phenomena that can be studied with underwater SPIV. The main contribution of this technique is in the field of wave kinematics, viscosity study, as well as the characteristics of the turbulence in the flow around the floaters. Hydrodynamical phenomena related to floater design and their degree of importance are outlined in Table 1, which are based on studies in the OC5 project (Robertson et al., 2017), (Amy Robertson, n.d.).

370

**Table 1** The hydrodynamical phenomenon ident. ranking based on OC5 project (H: High, M: Medium, L: Low)

Row	Phenomena	Importance	Physics Understanding	Validation Needs	Suitability of underwater S-PIV for providing validation data
1	VIV/VIM - substructure	M	L	H	Yes
2	Nonlinear excitation – diff/sum/mean	H	M	H	Yes
3	Short-crested waves	M	H	H	Yes
4	Marine growth influence on loads	L	H	L	Yes
5	Breaking/steep wave loads	L	M	H	Yes
6	Wave-current body interaction	H	M	M	Yes
7	Viscous load model	H	M	H	Yes
8	Multi-body flow interaction	H	M	H	Yes

**4.1 Vortex induced vibration and motion**

One field of the S-PIV contribution to FOWTs design is to study the vorticity field behind the model. This could be beneficial to study problems such as vortex-induced vibrations and motions. An experimental of flow-induced oscillations of a floating model spar-type floater is conducted by Carlson (Carlson and Modarres-Sadeghi, 2018). The model was the 1:470 scale of Hywind spar platform. In this study, the amplitude and frequency of the platform response is captured by tracker cameras. Moreover, wake visualisation was carried out by snap shooting of smoke behind the model. Using S-PIV in this type of study could be beneficial since the vorticity core in Z direction (normal to the water surface) can be captured, and this can be done in for different shedding frequencies. Then, the trajectory of these vortexes and their excitation region can be identified. This valuable data can then be used to

375

380



minimising the VIV effect, as well as analysing different VIV suppression methods, for instance, for reviewing different strake shapes on the model.

## 385 **4.2 Nonlinear wave loads**

The S-PIV result could be used to study of the Nonlinear wave effects on the floater, as the linear wave assumption has considerable error for wave loading and the platform response estimation. Among the ongoing research, the conducted research by (Pan and Ishihara, 2018) can be mentioned. In this research, the effect of nonlinear assumption for motion analysing of FOWT with a Semisubmersible floater is reviewed. It is shown that compared to nonlinear waves, linear wave theory has an overestimation of 17.6% for pitch and 24.6% for heave responses of the platform.

A study on the effects of fully nonlinear wave loads on FOWTs is conducted in press (Xu et al., 2019). In this study the effect of linear and fully nonlinear wave loads on OC4 semi-submersible platform is examined. The focus of research was mainly on floater motion, structural responses, as well as mooring line tension due to nonlinear and linear waves. The parameter that takes into account was the wave free-surface location and velocity distribution near the platform. Other results that were study were included the wave spectrum at different frequency range. The S-PIV method can make a great contribution here, since it is an instantaneous and visual method, these results can be visualised and examined simultaneously.

Floating wind turbine is a complex system and the motion of the supporting platform, as well as the turbine performance are coupled. Having an appropriate understanding of nonlinear wave excitation on floater could be useful to estimate the wave loading on the floater, as well as floater responses in different sea state. This understanding can later be used to optimise the turbine control system. This optimal control system needs to have efficiency for disturbance rejection and load reduction on turbine. A review on the state of the art of the control strategy for FOWT is carried out by (Salic et al., 2019). Another note about FOWTs is the LCOE. From control point of view, the control system should operate turbine near its optimum operation point against different transient and steady state aero and hydrodynamic loading conditions. In realistic sea state, nonlinear waves cause critical floater responses in terms of critical floater motion, mooring responses, as well as wave elevation around the platform. Providing data with S-PIV to study on the nonlinear wave effect, as well as possible load cases, can later be use for designing reliable turbine controller systems, better turbine efficiency, and lower LCoE.



#### 410 **4.3 Short-crested waves**

In comparison to slender members of Jacket platforms, the sub-structure of a FOWT is a large-scale bluff body. So that the presence of substructure in the incident waves, make scattered waves in the vicinity area. As a classical approach, the diffraction theory can use to study the hydrodynamics of these bluff body in waves. Moreover, boundary element method can use to solve this diffraction of waves. Diffraction theory is widely used for solving linear plane waves around hydrodynamically bluff body; the experimental validation for this method can find in literature (Chakrabarti and Tam, 1975). As discussed by (Hedges et al., 1993), although the diffraction theory is a practical approach to model wind generated waves, these waves are modelled more realistic with Short-crested waves. Application of short crested waves are the matter of interest for many researchers (Wang et al., 2019), (Wei and Dalrymple, 2017), (Vasarmidis et al., 2019).

420 Variety of study on short-crested waves is conducted in literature, one of which is the experimental study on directional hydrodynamic coefficient and wave force due to spreading angles of these waves (Ng et al., 2020). In this study the wave surface elevation, as well as force exerted on a cylinder model is studied. Range of 0 to 45 degrees is considered for directional spreading angles. Then, the relation of this parameter with Keulegan-Carpenter (KC) number is reviewed. Main result of this study is the wave time history, wave elevation, and wave force on the model, regarding the spreading angles. Drag and inertia coefficient is extracted. Moreover, the effect of short-crested waves on the wave force is studied. From the optical perspective, S-PIV can have an indirect contribution for study of short-crested waves. Although, this method can not be used for direct measurements of applied forces, as well as drag and inertia coefficient; the wave elevation and surface level change can be extracted in real time. Having the turbulent contours, velocity field and pressure field in this elevation studied, could easily help to identify the applied forces. Although, for studding the FOWT in wave tank, sensors such as Tri-axial accelerometer, Inertia motion unit, and different load cells are practical equipment. For the study of wave kinematics and dynamics, researchers can only use resistive wave gauges, current profiler, as well as Aquadopp, which are sampling the data in some point. The S-PIV can be useful to study the short-crested waves, as it brings instantaneous field contour srelated to study wave kinematic.

435

#### **4.4 Marine growth influence on loads**

There are strong ways for S-PIV contribution to study Marine growth effect on FOWTs. Marine growth could have different effects on the substructure of FOWTs. It is mainly caused to increase the thickness, structural weigh, drag



440 coefficient, as well as hydrodynamical added mass of the platform. The effect of marine growth on dynamics of  
offshore wind support structures is studied by many researchers, from which the conducted research by (Martinez-  
Luengo et al., 2017) can be mentioned. In this research a special focus is set to the effect of zonation and thickness  
of marine growth on mode shapes, as well as natural and bucking frequencies of supporting platform. In order to  
estimate the wave force, drag and inertia coefficient are calculated only based on offshore standards and guidelines  
(DNV-OS-J101, 2014), (API 2A-WSD, 2014). The main variation of drag and inertia coefficient due to marine  
445 growth is related to thickness and distribution of the growth, Keulegan-Carpenter number, relative surface tension,  
along with direction of incident waves. The drag component integration can be conduct with S-PIV method.

This drag interrogation could be align with inflow, crossflow, as well as specific directions, for instance align with  
vortex drags. This result could be used to study marine growth effect on the floater drag coefficient with different  
feasible growth thickness and distribution. Since the result are based on quantitative optic measurement, it can also  
450 be used to study the turbulence and vortexes generation of marine growth on the floater.

The S-PIV experiments could be used to study the marine growth effect on tendon and mooring line responses. The  
marine growth has influence on the mooring lines and umbilical cables. This could happen by incising their  
diameter. Although in practice this thickness increase is considered as an ideal and homogeneous roughness, studies  
are shows that this idealisation is not valid for realistic condition in the sea. In realistic situation, a great portion of  
455 marine growth could be attached to specific potion of mooring lines. A research on effect of marine growth on  
FOWTs mooring lines is carried out in press (Pham et al., 2017); in which the dynamic behaviour of mooring lines  
under the effect of quantity and the distribution of marine growth is studied. In this research, different distribution  
of marine growth is considered, and for each test case, the tensions and effective tension in Anchor and Fairlead  
points is investigated. In literature (Chuang et al., 2021), conventional equipment such as load cells is mainly used  
460 to study the FOWT's mooring line responses. However, the S-PIV can also have a contribution to this topic.

The point is that different materials can be used for FOWTs mooring, for lines, such as synthetic ropes, chains, and  
wire ropes. This material could have a different effect on marine growth, such as different intensities or distribution  
of growth on them. S-PIV could be utilised along with loadcells, so meanwhile that the tension in both failed and  
the anchor is provided, the main parameters of marine growth on a mooring can be examined in interrogation  
465 windows along the mooring length. These turbulent parameters could be the parameters such as Wake Vortex  
Turbulence, turbulence energy, and q criterion. Moreover, in the case of using the tendon, the VIV of the mooring  
could be investigated.



#### 4.5 Breaking/steep wave loads

470 A important field that S-PIV can play a role is to quantitative estimation of the breaking/steep wave loading on the  
FOWTs. When breaking wave occurs, a mixture of air and water create a turbulent flow region. This air-sea  
interface has a complex structure. Regarding the research that is carried out to the date (van der A et al., 2017), the  
accurate shape and loading of breaking waves is not achieved in literature. Laboratory research on breaking wave  
in deep water is conducted (Ticona Rollano et al., 2019), which was maily focused on wave breaking rates and  
wave-following turbulent dissipation. There is also some effort in literature to simulate this phenomena effect on  
475 fixed and moored floating with SPH<sup>1</sup> method (Liu et al., 2019). However, as these resercaher reviewed, the  
magnitude of this phenomena is overestimated by 30% in numerical cases.

The S-PIV could be beneficial here, since it could help to extract instantaneous velocity components and vectors  
for each sequence of breaking wave. Then, other related parameters of turbulent such as time-dependent turbulent  
kinetic energy, Reynolds Stress, as well as turbulent production, and dissipation could extracted.

480

#### 4.6 Wave-current body interaction

Interaction of gravity waves and surface mean flow could have a complex structure, which S-PIV could be utilised  
to investigate this phenomenon. Current could act as a damping source for long structures (Ye and Ji, 2019).  
Moreover, the current made frequency shift and shape modification to the wave; hence, the interaction of the  
485 incident current and waves to the structure could be the matter of interest in FOWT motion analysis. Research is  
carried on the wave-current interaction effect on a 5MW FOWT with OC3-Hywind spar floater (Chen and Basu,  
2019). In this research, FOWT response under waves with and without current interaction is studied. The result  
was mainly tower displacement, floater displacements, as well as mooring tensions at Fairlead. In this research, it  
is showed that the simple method of superposing the wave and current effect causes the overestimation in the  
490 response of the FOWT. This difference causes the overestimation of 12% in mooring tension force. The S-PIV  
could be used for the study of wave kinematic with and without current interaction; the S-PIV velocity and verticity  
results on this complex turbulent structure could be used for different wave and current propagation angles.  
Moreover, the floater wave-making in that load cases can be review quantitatively.

---

<sup>1</sup> Smoothed-particle hydrodynamics



#### 4.7 Viscous load model

495 The viscous loads are an important load case in FOWTs analysis, since the viscosity could have different effects on the floater. Among the different phenomena caused by viscosity, the viscous drift forces in extreme sea states (Tan et al., 2021), as well as viscous damping<sup>1</sup> effect (Clement et al., 2021) on floater and mooring line could be mentioned. The point is that the FOWTs models with second-order potential-flow theory usually shows underestimate forces and results, comparing to CFD and lab testing approach (Wang et al., 2021a). This is mainly  
500 because of ignoring the separation and viscous drag in potential-flow theory.

As it is proven in literature, the viscosity field for a pseudoplastic flow could be captured with S-PIV method (Tiwari et al., 2021). This research is interesting since the both momentum conservation, and equation and rheological model are replaced with S-PIV data. Therefore, the viscosity field is examined indirectly. Moreover, it is shown the well known approach in determining the viscosity effects, such as the power law and Carreau-Yasuda model,  
505 results in unrealistic increase in viscosity estimation. These kinds of research could be established for studying of FOWTs and Newtonian fluid. Notably the wake structure and share of pressure, viscosity and kinetic energy in this structure could be visualized and examined.

#### 4.8 Multi-body flow interaction

510 The S-PIV result could also have a contribution in developing other novel approaches in FOWTs analysis, for instance multibody modelling. Many researches are carried out in terms of utilising the multibody method for FOWTs analysis, for example (Lemmer et al., 2020), (Ma et al., 2019), and (Al-Solihat and Nahon, 2018); meanwhile some research was mainly focused on coupling this method with numerical methods such as potential theory and CFD (Ma et al., 2019). The S-PIV could have an important, though indirect, contribution in this field. Since the multibody approach  
515 is usually coupled with numerical models, such as CFD or BEM method, the S-PIV data could act as a replacement or validation source for hydrodynamic data. A research on uncertainty of CFD method for analysis of FOWTs is conducted in literature (Wang et al., 2021b). In this research, as the researchers examined, the total uncertainty of CFD for estimating the difference-frequency heave force is in the order of 51 percent. Using the underwater S-

---

<sup>1</sup> Also known as eddy making damping



PIV data, instead of the CFD for coupling with multibody method, could mitigate the relevant errors and  
520 uncertainties.

## 5 Conclusions

There is a need for high-fidelity data to aid the development of the emerging numerical tools and for validation of  
the new CFD and SPH codes. This paper has presented a review of the use of S-PIV in tank testing campaigns. The  
S-PIV technique and the technology used have been described, and its application in the fields of marine and  
525 offshore engineering has been discussed. It is also discussed that Underwater S-PIV has been used for the  
hydrodynamical study of other marine and offshore applications, including ship models, tidal stream turbines and  
propellers. However, the use of S-PIV for hydrodynamic of FOWTs is an emerging field.

It has been discussed that when tank tests only use pitot tube, wave probs and doppler sensors, the hydrodynamical  
results were generally limited to a certain point that these equipment are installed. Additionally, the use of these  
530 instruments results in more manipulation of the fluid flow and measurements error. As an alternative, fluid flow  
measurement can be conducted with underwater S-PIV. It has been shown that there is a gap between state of the  
art in tank testing and the demand for new numerical tools. A suitable method to improve the level of experimental  
campaigns is to combine them with the S-PIV method. The underwater S-PIV approach can easily fill this gap, and  
with its use, the unsteady structure of turbulent flow around the floater can be measure and understand.

S-PIV is an underutilised technique in FOWT design and has the capacity to provide critical validation data for  
535 high fidelity numerical tools. Such data and validated tools will contribute to our understanding of hydrological  
phenomenon such as those which have been identified by OC5 project as contributing to uncertainty in the design  
of floating offshore wind turbines. With established best practice guidelines, S-PIV can make a significant  
contribution to the reduction of uncertainty and ultimate the cost of FOWT.

In the continuation of the current study, the most critical points related to the application of this method in a tank  
540 test, moreover its errors and uncertainties, were examined. Additionally, in the current study, the important  
phenomena related to the hydrodynamic of FOWTs were addressed. As discussed, the underwater S-PIV method  
is a practical tool to investigate and measure these phenomena. The high-resolution data of the S-PIV later can be  
used as a validation source for the numerical tools in the field.



## 545 **Acknowledgements**

This research has received funding from the European Union's Horizon 2020 research and innovation programme under the Marie Skłodowska-Curie grant agreement N° 860879.

## **References**

550 van der A, D. A., van der Zanden, J., O'Donoghue, T., Hurther, D., Cáceres, I., McLelland, S. J. and Ribberink, J. S.: Large-scale laboratory study of breaking wave hydrodynamics over a fixed bar, *J. Geophys. Res. Ocean.*, 122(4), 3287–3310, doi:<https://doi.org/10.1002/2016JC012072>, 2017.

Abdulwahab, M., Ali, Y., Habeeb, F., Borhana, A., Abdelrhman, A. and Al-Obaidi, S.: *A Review in Particle Image Velocimetry Techniques (Developments and Applications)*, 2020.

555 Adrian, R. J. and Westerweel, J.: *Particle Image Velocimetry*, Cambridge University Press. [online] Available from: <https://trove.nla.gov.au/work/38209337>, 2011.

Adrian, L., Adrian, R. J. and Westerweel, J.: *Particle Image Velocimetry*, Cambridge University Press. [online] Available from: <https://books.google.ie/books?id=jbDI2-yHbooC>, 2011.

Ajay K. Prasad: *Particle Image Velocimetry*, *Curr. Sci.*, 79(1), 2000.

560 Al-Muhammad, J., Tomas, S., Ait-Mouheb, N., Amielh, M. and Anselmet, F.: Micro-PIV characterization of the flow in a milli-labyrinth-channel used in drip irrigation, *Exp. Fluids*, 59(12), 181, doi:10.1007/s00348-018-2633-x, 2018.

Al-Solihat, M. K. and Nahon, M.: Flexible Multibody Dynamic Modeling of a Floating Wind Turbine, *Int. J. Mech. Sci.*, 142–143, 518–529, doi:10.1016/j.ijmecsci.2018.05.018, 2018.

565 Amy Robertson: *Integrated Systems Design and Analysis Offshore Wind Project ID #T10*. [online] Available from: [https://www.energy.gov/sites/prod/files/2019/05/f63/T10 - Robertson\\_0.pdf](https://www.energy.gov/sites/prod/files/2019/05/f63/T10 - Robertson_0.pdf), n.d.

Anthony F. Molland: *The Maritime Engineering Reference Book - Underwater vehicles*, pp. 728–783, Elsevier., 2008.

API 2A-WSD: *Planning , Designing , and Constructing Fixed Offshore Platforms — Working Stress Design.*, 2014.

570 Ashworth Briggs, A., Fleming, A., Duffy, J. and Binns, J. R.: Tracking the vortex core from a surface-piercing flat plate by particle image velocimetry and numerical simulation, *Proc. Inst. Mech. Eng. Part M J. Eng. Marit.*



- Environ., 233(3), 793–808, doi:10.1177/1475090218776202, 2019.
- Baghaie, A.: Robust Principal Component Analysis for Background Estimation of Particle Image Velocimetry Data, in 2019 IEEE Long Island Systems, Applications and Technology Conference (LISAT), pp. 1–6., 2019.
- 575 Bayati, I., Bernini, L., Zanotti, A., Belloli, M. and Zasso, A.: Experimental investigation of the unsteady aerodynamics of FOWT through PIV and hot-wire wake measurements, *J. Phys. Conf. Ser.*, 1037(5), doi:10.1088/1742-6596/1037/5/052024, 2018.
- Bhattacharya, S., Charonko, J. and Vlachos, P.: Particle Image Velocimetry (PIV) Uncertainty Quantification Using Moment of Correlation (MC) Plane., 2018.
- Carlson, D. W. and Modarres-Sadeghi, Y.: Vortex-induced vibration of spar platforms for floating offshore wind  
580 turbines, *Wind Energy*, 21(11), 1169–1176, doi:10.1002/we.2221, 2018.
- Catipovic, M. A., Tyler, P. M., Trapani, J. G. and Carter, A. R.: Improving the quantification of Brownian motion, *Am. J. Phys.*, 81(7), 485–491, doi:10.1119/1.4803529, 2013.
- Chakrabarti, S. K. and Tam, W. A.: Interaction of Waves with Large Vertical Cylinder, *J. Sh. Res.*, 19(01), 23–33, doi:10.5957/jsr.1975.19.1.23, 1975.
- 585 Chaouat, B.: The State of the Art of Hybrid RANS/LES Modeling for the Simulation of Turbulent Flows, *Flow, Turbul. Combust.*, 99(2), 279–327, doi:10.1007/s10494-017-9828-8, 2017.
- Charonko, J. J. and Vlachos, P. P.: Estimation of uncertainty bounds for individual particle image velocimetry measurements from cross-correlation peak ratio, *Meas. Sci. Technol.*, 24(6), 65301, doi:10.1088/0957-0233/24/6/065301, 2013.
- 590 Chen, L. and Basu, B.: Wave-current interaction effects on structural responses of floating offshore wind turbines, *Wind Energy*, 22(2), 327–339, doi:10.1002/we.2288, 2019.
- Chen, P., Chen, J. and Hu, Z.: Review of Experimental-Numerical Methodologies and Challenges for Floating Offshore Wind Turbines, *J. Mar. Sci. Appl.*, 19(3), 339–361, doi:10.1007/s11804-020-00165-z, 2020.
- Choi, S., Kim, W., Côté, D., Park, C.-W. and Lee, H.: Blood cell assisted in vivo Particle Image Velocimetry using  
595 the confocal laser scanning microscope, *Opt. Express*, 19, 4357–4368, doi:10.1364/OE.19.004357, 2011.
- Chong, K. L., Shi, J. Q., Ding, G. Y., Ding, S. S., Lu, H. Y., Zhong, J. Q. and Xia, K. Q.: Vortices as Brownian



particles in turbulent flows, *Sci. Adv.*, 6(34), 1–8, doi:10.1126/sciadv.aaz1110, 2020.

Chuang, T. C., Yang, W. H. and Yang, R. Y.: Experimental and numerical study of a barge-type FOWT platform under wind and wave load, *Ocean Eng.*, 230(November 2020), 109015, doi:10.1016/j.oceaneng.2021.109015, 2021.

Clement, C., Kosleck, S. and Lie, T.: Investigation of viscous damping effect on the coupled dynamic response of a hybrid floating platform concept for offshore wind turbines, *Ocean Eng.*, 225, 108836, doi:<https://doi.org/10.1016/j.oceaneng.2021.108836>, 2021.

Cordle, A. and Jonkman, J.: State of the art in floating wind turbine design tools, *Proc. Int. Offshore Polar Eng. Conf.*, (October), 367–374, 2011.

Day, A. H., Babarit, A., Fontaine, A., He, Y. P., Kraskowski, M., Murai, M., Penesis, I., Salvatore, F. and Shin, H. K.: Hydrodynamic modelling of marine renewable energy devices: A state of the art review, *Ocean Eng.*, 108, 46–69, doi:10.1016/j.oceaneng.2015.05.036, 2015.

Desmond, C., Murphy, J., Blonk, L. and Haans, W.: Description of an 8 MW reference wind turbine, *J. Phys. Conf. Ser.*, 753(9), doi:10.1088/1742-6596/753/9/092013, 2016.

Desmond, C. J., Watson, S. J., Aubrun, S., Ávila, S., Hancock, P. and Sayer, A.: A study on the inclusion of forest canopy morphology data in numerical simulations for the purpose of wind resource assessment, *J. Wind Eng. Ind. Aerodyn.*, 126, 24–37, doi:<https://doi.org/10.1016/j.jweia.2013.12.011>, 2014.

DNV-OS-J101: Design of Offshore Wind Turbine Structures. [online] Available from: <https://rules.dnvgl.com/docs/pdf/dnv/codes/docs/2014-05/os-j101.pdf>, 2014.

DNV GL: Floating Wind: the Power To Commercialize. [online] Available from: [www.dnvgl.com](http://www.dnvgl.com), 2020.

Dong, R. R., Katz, J. and Huang, T. T.: On the structure of bow waves on a ship model, *J. Fluid Mech.*, 346, 77–115, doi:10.1017/S0022112097005946, 1997.

Egeberg, T. F., Yoon, H., Stern, F., Pettersen, B. and Bhushan, S.: Vortex shedding from a ship hull by means of tomographic PIV, *Proc. Int. Conf. Offshore Mech. Arct. Eng. - OMAE*, 8A(Dtmb 5415), doi:10.1115/OMAE2014-23357, 2014.

Fuentes-Pérez, J. F., Meurer, C., Tuhtan, J. A. and Kruusmaa, M.: Differential Pressure Sensors for Underwater Speedometry in Variable Velocity and Acceleration Conditions, *IEEE J. Ocean. Eng.*, 43(2), 418–426,



doi:10.1109/JOE.2017.2767786, 2018.

625 Garcia, D.: A fast all-in-one method for automated post-processing of PIV data, *Exp. Fluids*, 50(5), 1247–1259, doi:10.1007/s00348-010-0985-y, 2011.

Go, S. C., Seo, J., Park, J. and Rhee, S. H.: Towed underwater PIV measurement of propeller wake in self-propelled condition, *Exp. Fluids*, 60(12), 1–16, doi:10.1007/s00348-019-2827-x, 2019.

635 Grizzi, S., Pereira, F. and Di Felice, F.: A simplified, flow-based calibration method for stereoscopic PIV, *Exp. Fluids*, 48(3), 473–486, doi:10.1007/s00348-009-0750-2, 2010.

Han, B. W., Seo, J., Lee, S. J., Seol, D. M. and Rhee, S. H.: Uncertainty assessment for a towed underwater stereo PIV system by uniform flow measurement, *Int. J. Nav. Archit. Ocean Eng.*, 10(5), 596–608, doi:10.1016/j.ijnaoe.2017.11.005, 2018.

635 Hedges, T. S., Tickell, R. G. and Akrigg, J.: Interaction of short-crested random waves and large-scale currents, *Coast. Eng.*, 19(3), 207–221, doi:[https://doi.org/10.1016/0378-3839\(93\)90029-8](https://doi.org/10.1016/0378-3839(93)90029-8), 1993.

Ismadi, M.-Z., Higgins, S., Samarage, C. R., Paganin, D., Hourigan, K. and Fouras, A.: Optimisation of a Stirred Bioreactor through the Use of a Novel Holographic Correlation Velocimetry Flow Measurement Technique, *PLoS One*, 8(6), e65714 [online] Available from: <https://doi.org/10.1371/journal.pone.0065714>, 2013.

640 ITTC: Uncertainty Analysis Particle Imaging Velocimetry. [online] Available from: <https://itc.info/media/1211/75-01-03-03.pdf>, 2008.

Jacobi, G., Thill, C. H. and Huijsmans, R. H. M.: The application of particle image velocimetry for the analysis of high-speed craft hydrodynamics, *ICHHD 2016 12th Int. Conf. Hydrodyn.* [online] Available from: <https://repository.tudelft.nl/islandora/object/uuid%3Abe0cb492-12fc-4aa5-8abc-abd6cf8ff762>, 2016.

645 Jurgens, A.: EXPERIMENTAL INVESTIGATION INTO THE FLOW AROUND A MANOEUVRING LNG CARRIER ON SHALLOW WATER., 2007.

Jux, C., Sciacchitano, A., Schneiders, J. and Scarano, F.: Robotic volumetric PIV of a full-scale cyclist, *Exp. Fluids*, 59, doi:10.1007/s00348-018-2524-1, 2018.

Kähler, C., Cierpka, C. and Scharnowski, S.: On the uncertainty of digital PIV and PTV near walls, *Exp. Fluids*, 52, 1641–1656, doi:10.1007/s00348-012-1307-3, 2012.



- 650 Keane, R. D. and Adrian, R. J.: Theory of cross-correlation analysis of PIV images, *Appl. Sci. Res.*, 49(3), 191–215, doi:10.1007/BF00384623, 1992.
- Lee, J. Y., Paik, B. G. and Lee, S. J.: PIV measurements of hull wake behind a container ship model with varying loading condition, *Ocean Eng.*, 36(5), 377–385, doi:10.1016/j.oceaneng.2009.01.006, 2009.
- Lee, S. K., Giacobello, M., Manovski, P. and Kumar, C.: Optimising camera arrangement for stereoscopic particle  
655 image velocimetry, *Proc. 19th Australas. Fluid Mech. Conf. AFMC 2014*, (December), 8–11, 2014.
- Lemmer, F., Yu, W., Luhmann, B., Schlipf, D. and Cheng, P. W.: Multibody modeling for concept-level floating offshore wind turbine design, *The Author(s)*., 2020.
- Liu, S., Ong, M. and Obhrai, C.: Numerical Simulations of Breaking Waves and Steep Waves Past a Vertical Cylinder at Different Keulegan–Carpenter Numbers, *J. Offshore Mech. Arct. Eng.*, 141, doi:10.1115/1.4043278,  
660 2019.
- Liu, Y., Xiao, Q., Incecik, A., Peyrard, C. and Wan, D.: Establishing a fully coupled CFD analysis tool for floating offshore wind turbines, *Renew. Energy*, 112, 280–301, doi:10.1016/j.renene.2017.04.052, 2017.
- Liu, Z., Jia, L., Zheng, Y. and Zhang, Q.: Flow-adaptive data validation scheme in PIV, *Chem. Eng. Sci.*, 63, 1–11, doi:10.1016/j.ces.2007.08.080, 2008.
- 665 Ma, Z., Wang, S., Wang, Y., Ren, N. and Zhai, G.: Experimental and numerical study on the multi-body coupling dynamic response of a Novel Serbuoys-TLP wind turbine, *Ocean Eng.*, 192(July 2018), 106570, doi:10.1016/j.oceaneng.2019.106570, 2019.
- Mallat, B., Germain, G., Delacroix, S., Druault, P., Dussol, D. and Billard, J.-Y.: PIV measurements around a ship bow., 2015.
- 670 Markus, Raffel. Christian E. Willert, Fulvio Scarano, C. J.: *Particle Image Velocimetry: A Practical Guide*, 3rd ed., Springer., 2018.
- Martinez-Luengo, M., Causon, P., Gill, A. B. and Kolios, A. J.: The effect of marine growth dynamics in offshore wind turbine support structures, in *6th International Conference on Marine Structures, MARSTRUCT 2017*, edited by S. C.G. and G. Y., pp. 889–898, CRC Press/Balkema, Centre for Offshore Renewable Energy Engineering,  
675 School of Water, Energy and Environment, Cranfield University, Cranfield, United Kingdom., 2017.
- Neal, D., Sciacchitano, A., Smith, B. and Scarano, F.: Collaborative framework for PIV uncertainty quantification:



The experimental database, *Meas. Sci. Technol.*, 26, doi:10.1088/0957-0233/26/7/074003, 2015.

Ng, C. Y., Tuhaijan, S. N. A., Fattah, M. Z. A., John Kurian, V. and Mustaffa, Z.: Experimental investigation of directional hydrodynamic coefficients and the effects on wave force due to spreading angles, *Ain Shams Eng. J.*, 11(4), 1021–1034, doi:10.1016/j.asej.2020.01.012, 2020.

Olsen, M. G. and Adrian, R. J.: Brownian motion and correlation in particle image velocimetry, *Opt. Laser Technol.*, 32(7–8), 621–627, doi:10.1016/S0030-3992(00)00119-5, 2000.

Otter, A., Pakrashi, V., Robertson, A., Murphy, J. and Desmond, C.: Review of modelling techniques for floating offshore wind turbines, *Wind Energy*, 2021.

Pan, J. and Ishihara, T.: Nonlinear wave effects on dynamic responses of a semisubmersible floating offshore wind turbine in the intermediate water, *J. Phys. Conf. Ser.*, 1037(2), doi:10.1088/1742-6596/1037/2/022037, 2018.

Pham, H., Veritas, B., Arnal, V. and Nantes, E. C. De: Effect of Marine Growth on Floating Wind Turbines Mooring Lines Responses Abstract :, , (December), 2017.

Pun, C.-S., Susanto, A. and Dabiri, D.: Mode-ratio bootstrapping method for PIV outlier correction, *Meas. Sci. Technol.*, 18, 3511, doi:10.1088/0957-0233/18/11/035, 2007.

Rahimi, H., Dose, B., Stoevesandt, B. and Peinke, J.: Investigation of the validity of BEM for simulation of wind turbines in complex load cases and comparison with experiment and CFD, in *Journal of Physics: Conference Series*, vol. 749., 2016.

Rezaeiha, A., Montazeri, H. and Blocken, B.: On the accuracy of turbulence models for CFD simulations of vertical axis wind turbines, *Energy*, 180, 838–857, doi:10.1016/j.energy.2019.05.053, 2019.

Robertson, A. N., Wendt, F., Jonkman, J. M., Popko, W., Dagher, H., Gueydon, S., Qvist, J., Vittori, F., Azcona, J., Uzunoglu, E., Soares, C. G., Harries, R., Yde, A., Galinos, C., Hermans, K., De Vaal, J. B., Bozonnet, P., Bouy, L., Bayati, I., Bergua, R., Galvan, J., Mendikoa, I., Sanchez, C. B., Shin, H., Oh, S., Molins, C. and Debruyne, Y.: OC5 Project Phase II: Validation of Global Loads of the DeepCwind Floating Semisubmersible Wind Turbine, *Energy Procedia*, 137(January), 38–57, doi:10.1016/j.egypro.2017.10.333, 2017.

Salic, T., Charpentier, J. F., Benbouzid, M. and Boulluec, M. Le: Control strategies for floating offshore wind turbine: Challenges and trends, *Electron.*, 8(10), 1–14, doi:10.3390/electronics8101185, 2019.

Scharnowski, S. and Kähler, C.: On the loss-of-correlation due to PIV image noise, *Exp. Fluids*, 57, 119,



doi:10.1007/s00348-016-2203-z, 2016.

705 Schröder, A., Willert, C., Schanz, D., Geisler, R., Jahn, T., Gallas, Q. and Leclaire, B.: The flow around a surface mounted cube: a characterization by time-resolved PIV, 3D Shake-The-Box and LBM simulation, *Exp. Fluids*, 61(9), 1–22, doi:10.1007/s00348-020-03014-5, 2020.

Sciacchitano, A.: Uncertainty quantification in particle image velocimetry, *Meas. Sci. Technol.*, 30(9), doi:10.1088/1361-6501/ab1db8, 2019.

710 Seo, J., Lee, S. J., Choi, W. S., Park, S. T. and Rhee, S. H.: Experimental study on kinetic energy conversion of horizontal axis tidal stream turbine, *Renew. Energy*, 97, 784–797, doi:10.1016/j.renene.2016.06.041, 2016.

Tan, L., Ikoma, T., Aida, Y. and Masuda, K.: Mean Wave Drift Forces on a Barge-Type Floating Wind Turbine Platform with Moonpools, *J. Mar. Sci. Eng.*, 9(7), doi:10.3390/jmse9070709, 2021.

715 Ticona Rollano, F., Brown, A., Ellenson, A., Özkan-Haller, H. T., Thomson, J. and Haller, M. C.: Breaking waves in deep water: measurements and modeling of energy dissipation, *Ocean Dyn.*, 69(10), 1165–1179, doi:10.1007/s10236-019-01301-2, 2019.

Timmins, B., Wilson, B., Smith, B. and Vlachos, P.: A method for automatic estimation of instantaneous local uncertainty in particle image velocimetry measurements, *Exp. Fluids*, 53, 1133–1147, doi:10.1007/s00348-012-1341-1, 2012.

720 Tiwari, N., Tasaka, Y. and Murai, Y.: PIV-based estimation of viscosity and pressure fields for a steady pseudoplastic flow, *Flow Meas. Instrum.*, 77, 101852, doi:10.1016/j.flowmeasinst.2020.101852, 2021.

Tukker, J., Blok, J. J., Kuiper, G. and Huijsmans, R. H. M.: Wake Flow Measurements in Towing Tanks with PIV, *Proc. 9th Int. Symp. Flow Vis.*, (373), 1–12, 2000.

725 Vasarmidis, P., Stratigaki, V. and Troch, P.: Accurate and fast generation of irregular short crested waves by using periodic boundaries in a mild-slope wave model, *Energies*, 12(5), doi:10.3390/en12050785, 2019.

Wang, L., Robertson, A., Jonkman, J., Yu, Y.-H., Koop, A., Borràs Nadal, A., Li, H., Shi, W., Pinguet, R., Zhou, Y., Xiao, Q., Kumar, R. and Sarlak, H.: Investigation of Nonlinear Difference-Frequency Wave Excitation on a Semisubmersible Offshore-Wind Platform With Bichromatic-Wave CFD Simulations, *ASME 2021 3rd Int. Offshore Wind Tech. Conf.*, doi:10.1115/IOWTC2021-3537, 2021a.

730 Wang, L., Robertson, A., Jonkman, J. and Yu, Y. H.: Uncertainty assessment of CFD investigation of the nonlinear



difference-frequency wave loads on a semisubmersible FOWT platform, *Sustain.*, 13(1), 1–25, doi:10.3390/su13010064, 2021b.

Wang, P., Zhao, M. and Du, X.: Short-Crested Wave-Current Forces on Composite Bucket Foundation for an Offshore Wind Turbine, *Math. Probl. Eng.*, 2019, doi:10.1155/2019/5932742, 2019.

735 Wang, Z., Ozbay, A., Tian, W., Sharma, A. and Hu, H.: An experimental investigation on the wake characteristics behind a novel twin-rotor wind turbine, *33rd Wind Energy Symp.*, (January), 1–15, doi:10.2514/6.2015-1663, 2015.

Wei, Z. and Dalrymple, R. A.: SPH Modeling of Short-crested Waves, , (1) [online] Available from: <http://arxiv.org/abs/1705.08547>, 2017.

740 Westerweel, J., Elsinga, G. E. and Adrian, R. J.: Particle Image Velocimetry for Complex and Turbulent Flows, *Annu. Rev. Fluid Mech.*, 45(1), 409–436, doi:10.1146/annurev-fluid-120710-101204, 2013.

Wieneke, B.: PIV Uncertainty Quantification and Beyond, 21 December., 2017.

WindEurope: Floating offshore wind is gearing up for take-off. [online] Available from: <https://windeurope.org/newsroom/news/floating-offshore-wind-is-gearing-up-for-take-off/#>, 2020.

745 Wu, T., Deng, R., Luo, W., Sun, P., Dai, S. and Li, Y.: 3D-3C wake field measurement, reconstruction and spatial distribution of a Panamax Bulk using towed underwater 2D-3C SPIV, *Appl. Ocean Res.*, 105, 102437, doi:https://doi.org/10.1016/j.apor.2020.102437, 2020.

Xiao, J. P., Wu, J., Chen, L. and Shi, Z. Y.: Particle image velocimetry (PIV) measurements of tip vortex wake structure of wind turbine, *Appl. Math. Mech. (English Ed.)*, 32(6), 729–738, doi:10.1007/s10483-011-1452-x, 2011.

750 Xu, K., Shao, Y., Gao, Z. and Moan, T.: A study on fully nonlinear wave load effects on floating wind turbine, *J. Fluids Struct.*, 88, 216–240, doi:10.1016/j.jfluidstructs.2019.05.008, 2019.

Ye, K. and Ji, J.: Current, wave, wind and interaction induced dynamic response of a 5 MW spar-type offshore direct-drive wind turbine, *Eng. Struct.*, 178(August 2018), 395–409, doi:10.1016/j.engstruct.2018.10.023, 2019.

755 Yoon, H., Longo, J., Toda, Y. and Stern, F.: Benchmark CFD validation data for surface combatant 5415 in PMM maneuvers - Part II: Phase-averaged stereoscopic PIV flow field measurements, *Ocean Eng.*, 109, 735–750, doi:10.1016/j.oceaneng.2015.09.046, 2015.

<https://doi.org/10.5194/wes-2021-128>  
Preprint. Discussion started: 3 February 2022  
© Author(s) 2022. CC BY 4.0 License.



Zhong Li, Jinwei Ye, Yu Ji, Hao Sheng, J. Y.: PIV-Based 3D Fluid Flow Reconstruction Using Light Field Camera, Comput. Vis. Pattern Recognit., 2019.